INTERNATIONAL JOURNAL FOR NUMERICAL METHODS IN FLUIDS, VOL. 15, 219–232 (1992)

THE OSHER SCHEME FOR NON-EQUILIBRIUM REACTING FLOWS

AMBADY SURESH

Sverdrup Technology, Inc., NASA Lewis Research Center, Cleveland, OH 44135, U.S.A.

AND

MENG-SING LIOU

NASA Lewis Research Center, Cleveland, OH 44135, U.S.A.

SUMMARY

An extension of the Osher upwind scheme to non-equilibrium reacting flows is presented, Owing to the presence of source terms, the Riemann problem is no longer self-similar and therefore its approximate solution becomes tedious. With simplicity in mind, a linearized approach which avoids an iterative solution is used to define the intermediate states and sonic points. The source terms are treated explicitly. Numerical computations are presented to demonstrate the feasibility, efficiency and accuracy of the proposed method. The test problems include a ZND (Zeldovich–Neumann–Doring) detonation problem for which spurious numerical solutions which propagate at mesh speed have been observed on coarse grids. With the present method, a change of limiter causes the solution to change from the physically correct CJ detonation solution to the spurious weak detonation solution.

KEY WORDS Reacting flow Osher scheme Riemann solver ZND detonation

1. INTRODUCTION

Upwind schemes for solving the Euler equations of fluid dynamics have become very popular over the last decade owing to their excellent shock-capturing capabilities. Essentially, an upwind code consists of an interpolation procedure coupled with an approximate Riemann solver (ARS). Typically, the interpolation procedure reconstructs the variables within a computational cell, enforces some non-oscillatory constraint and necessarily introduces discontinuities at the cell interface. The role of the ARS is to evaluate the flux at the interface given the fluid states to the left and right of the interface. As the name suggests, this is done by solving a one-dimensional Riemann problem normal to the interface, an idea originally due to Godunov.[1] Since then a number of ARSs have become popular such as the Steger–Warming solver (SWS),[2] the van Leer solver (VLS),[3] the Roe solver (RS)[4] and the Osher solver (OS).[5]

The Osher solver,[5,6] which is the subject of this paper, has certain attractive features as compared to the other solvers. It is an extension of the Engquist–Osher[7] scheme for scalar hyperbolic conservation laws. The OS computes an interface flux which is a smooth function of the left and right states (which is not the case for the RS and SWS) and also statisfies the entropy inequality (in contrast to the RS which requires an entropy fix). On the other hand, its resolution on contact discontinuities is superior to the VLS and matches the resolution obtained with the

0271–2091/92/140219–14$12.00
© 1992 by John Wiley & Sons, Ltd.
Received 24 January 1991
Revised 25 October 1991

RS. For slowly moving shock waves Roberts[8] discovered that the OS gave the least post-shock oscillations of all these schemes. The main drawback of the OS seems to be its higher operation count and complexity in programming, which make it roughly 15%–60% more expensive than the RS. Despite this, it is our view that the superior qualities mentioned above make the extension of the OS to include general chemistry a worthwhile and useful thing to do.

Hypersonic flow is seeing a renewal of interest owing to advanced propulsion concepts such as the NASP, the Space Shuttle and future civil transport concepts. Such flows are generally accompanied by changes in the chemistry of the gas. It is here that upwind schemes with their excellent shock-capturing properties become invaluable. With the exception of the OS, all the above ARSs have been extended[9-13] to gases with a general equation of state and to gases in chemical non-equilibrium. This paper is a sequel to a previous paper of ours[14] in which the Osher scheme was extended to include gases with a general equation of state. Here we present an extension of the Osher scheme to flows which are in chemical non-equilibrium, i.e. where chemical reactions are taking place on the same time scale as the transit time of fluid particles. More precisely, if k denotes the reaction rate, L a characteristic length and u a characteristic velocity, we are concerned here with the case where the Damkohler number kL/u is of the order of unity. Examples of such flows include detonation phenomena, hypersonic flows of air and acoustic–flame interactions.

Upwind schemes for such flows, which are characterized by the presence of source terms on the right-hand side, have been developed and studied by several authors in recent times. LeVeque and Yee[15] study the effects of stiff source terms on scalar convection and observe incorrect speeds of propagation. Larrouturou and Fezoui[11] describe an extension of the Osher scheme to multi-species inert mixtures where the effects of chemical reactions are ignored. The extension of the Roe scheme[11,13] to such flows turns out to be a one-parameter family with no clear theoretical choice between them, although several work well in practice. Another approach is by Ben-Artzi,[16] who constructs an approximate solution to the generalized Riemann problem (GRP) (i.e. where the left and right states are piecewise linear) for such flows which is then used in a Godunov-type solver. Below we follow his notation and our second test problem is identical to his ZND detonation case.

In the rest of this paper we first discuss mixtures of perfect gases and reaction kinetics. In Section 3 we present the basic first-order explicit Osher scheme. A crucial element of this scheme is the determination of the intermediate states and sonic points, which are described in Section 4. In Section 5 we show how the results for the binary mixture can be easily extended to include an arbitrary number of species. Incorporation of these split flux formulae in a TVD algorithm and application to a few typical problems are described in Section 6 and our conclusions are to be found in Section 7.

2. PERFECT GAS MIXTURES

In this paper the fluid medium is assumed to be a mixture of perfect gases. The gas is assumed to be in thermal equilibrium, which implies the same temperature for all species. Diffusion effects are also neglected throughout the paper. For the kth species the mass fraction, molecular weight, specific heat at constant pressure and specific heat at constant volume will be denoted by z_k, M_k, C_{pk}, and C_{vk} respectively. By the perfect gas assumption C_{pk} and C_{vk} are constants and satisfy

$$M_k(C_{pk}-C_{vk})=R, \tag{1}$$

where R is the universal gas constant. If T and ρ denote the temperature and density of the mixture respectively, the total pressure p of the mixture is given by Dalton's law as

$$p=\sum_{k=1}^{n} p_k=\sum_{k=1}^{n} \frac{\rho z_k RT}{M_k}. \tag{2}$$

For hypersonic applications, chemical reactions are often accompanied by energy release. These are included in the specific internal energy of the mixture, which can be written as

$$e=\sum_{k=1}^{n} z_k(C_{vk}T+h_k^0), \tag{3}$$

where h_k^0 are the specific heats of formation. It is convenient to write equation (3) as

$$e=\hat{e}+\sum_{k=1}^{n} z_k h_k^0. \tag{4}$$

The pressure p can then be written as

$$p=(\gamma-1)\rho\hat{e}, \tag{5}$$

where γ stands for the ratio of specific heats of the mixture, given by

$$\gamma=\frac{\sum_{k=1}^{n} z_k C_{pk}}{\sum_{k=1}^{n} z_k C_{vk}}. \tag{6}$$

Note that γ is a function of z_i only. The rates of the chemical reactions can be written as

$$\frac{dz_i}{dt}=f_i(z_i, p, \rho), \tag{7}$$

where $\sum_{i=1}^{n} f_i=0$, since $\sum_{i=1}^{n} z_i=1$.

3. EULER EQUATIONS FOR REACTING FLOWS

For simplicity, we will first restrict ourselves to a binary mixture consisting of reactants and products and present the extension to several species in Section 5. Following the notation of Reference 16, $z_1=z$ denotes the mass fraction of the reactants, $1-z$ the mass fraction of the products and $f_1=-k(z, p, \rho)$ the reaction rate. The reaction is assumed to be irreversible, so that $k\geqslant 0$. Under these assumptions the 1D Euler equations take the form

$$\frac{\partial U}{\partial t}+\frac{\partial F(U)}{\partial x}=S(U), \tag{8}$$

where

$$U=[\rho, \rho u, \rho E, \rho z]^{\mathrm{T}}, \qquad F=[\rho u, \rho u^2+p, (\rho E+p)u, \rho uz]^{\mathrm{T}}, \qquad S=[0, 0, 0, -\rho k]^{\mathrm{T}}, \tag{9}$$

with $E=e+u^2/2$, $e=\hat{e}-z\Delta h+h_2^0$ and $\Delta h=h_2^0-h_1^0$ denotes the heat release.

The eigenvalues of the hyperbolic system given by (8) are

$$\lambda_1=u-a, \qquad \lambda_{2,3}=u, \qquad \lambda_4=u+a, \tag{10}$$

where a is given by

$$a^2=\gamma(z)p/\rho. \tag{11}$$

Equation (8) is spatially discretized in conservation form as

$$U_{it}+\frac{F_{i+1/2}-F_{i-1/2}}{\Delta x}=S_i. \tag{12}$$

In a Godunov-type scheme, when $S_i=0$, the interfacial flux $F_{i+1/2}$ is obtained by solving a Riemann problem locally between U_i and U_{i+1} and the value of $F_{i+1/2}$ is simply the value of the flux on the t-axis. In the Osher scheme using the natural order, this is done approximately by connecting U_i to U_{i+1} via a sequence of simple waves. This solution is exact when shocks are absent and is second-order-accurate for weak shocks, because the transition via compression waves and the transition through weak shocks differ only by terms third-order in the shock strength. For strong shocks this is still a good initial guess for the iterative exact solution. The formula for $F_{i+1/2}$ in the Osher scheme which results is

$$F_{i+1/2}=\tfrac{1}{2}(F_i+F_{i+1})-\tfrac{1}{2}\int_{U_i}^{U_{i+1}}|A|\,\mathrm{d}U, \tag{13}$$

where $|A|=A^+-A^-$ is the matrix based on the absolute value of the flux Jacobian and the integration is carried out along the sequence of simple waves shown in Figure 1. The advantage of this path is that once the intermediate states and the sonic points are known, the integral can be evaluated in closed form. For example, along a wave from U_L to U_R corresponding to a non-degenerate eigenvalue, the integral is

$$\int_{U_L}^{U_R}A^+\mathrm{d}U=\begin{cases}F(U_R)-F(U_L) & \text{if } \lambda(U_R)>0, \quad \lambda(U_L)>0,\\ F(U_R)-F(U_s) & \text{if } \lambda(U_R)>0, \quad \lambda(U_L)\leqslant 0,\\ F(U_s)-F(U_L) & \text{if } \lambda(U_R)\leqslant 0, \quad \lambda(U_L)>0,\\ 0 & \text{if } \lambda(U_R)\leqslant 0, \quad \lambda(U_L)\leqslant 0,\end{cases} \tag{14}$$

where U_s is the unique sonic point between U_R and U_L. Similarly, if the wave corresponds to a degenerate eigenvalue, then the integral is

$$\int_{U_L}^{U_R}A^+\mathrm{d}U=\begin{cases}F(U_R)-F(U_L) & \text{if } \lambda(U_R)=\lambda(U_L)>0,\\ 0 & \text{if } \lambda(U_R)=\lambda(U_L)\leqslant 0,\end{cases} \tag{15}$$

Thus equation (13) reduces to a sum of integrals of the form (14) and (15) over the various intermediate points. From a flux-difference-splitting point of view it is also possible to interpret

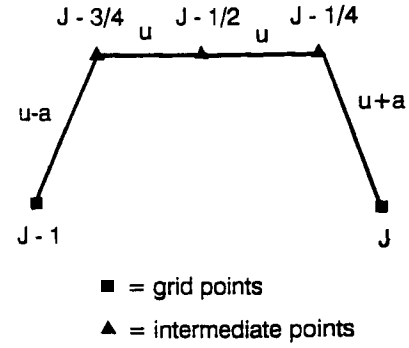

Figure 1. Schematic representation of the integration paths in the Osher scheme for reacting flow

these integrals as positive and negative flux differences. Thus the positive flux difference denoted by $\Delta^+ F_i^+$ is defined as

$$\Delta^+ F_i^+ = \int_{U_i}^{U_{i+1}} A^+ \mathrm{d}U$$

and is a sum of three integrals of the form (14) and (15). Similarly,

$$\Delta^+ F_i^- = \int_{U_i}^{U_{i+1}} A^- \mathrm{d}U$$

is the negative flux difference between i and $i+1$. These flux differences are used in the extension to second order presented below.

Owing to the inhomogeneous source term, the Riemann problem for (8) is no longer self-similar, i.e. the wavefronts are not rays through the origin. Thus, within the framework of Godunov schemes the interfacial flux is not constant on the t-axis but varies along it. To correctly account for the source term, it is also necessary to consider at least piecewise *linear* distributions of the data, since constant data are no longer in equilibrium. This is in fact the approach of Ben-Artzi,[16] who constructs an approximate solution for GRP in the vicinity of the origin and uses this solution to derive the interfacial flux.

In contrast, we wish to follow the simpler procedure of solving the Riemann problem as though the source terms were absent (called the associated Riemann problem (ARP)) and then adding in the source terms before advancing to the next time step. While it is quite clear that such a procedure neglects the interactions between acoustic waves and chemical reactions, it is also true that the source terms do not change the basic wave configuration at the singularity. This means that, for example, if the ARP has an S–C–R pattern, then so does the GRP. Moreover, along any fixed direction from the origin the solution to the GRP approaches the solution to the ARP sufficiently close to the origin (Prop. 7 of Reference 16). Thus, at least for relatively small source terms, the ARP can be used to resolve the discontinuity and the effects of the source terms added later. This is the rationale for the present approach.

In solving the Riemann problem for the homogenous system, the fluid is essentially treated as an inert mixture, similar to Larrouturou and Fezoui.[11] A significant difference is that in their approach the intermediate states can be obtained only iteratively. Even with a very good guess, this leads to an inefficient algorithm. In contrast, the intermediate states are obtained in the present method without any iteration, thus resulting in an efficient algorithm.

4. INTERMEDIATE STATES AND SONIC POINTS

As a first step towards deriving the intermediate points and sonic points, the eigenvectors along the various subpaths need to be derived. For convenience we prefer to use the primitive variables p, ρ, u and z. Along a simple wave corresponding to λ_1 we have

$$\frac{\mathrm{d}V}{\mathrm{d}\tau} = e_1,$$

where

$$V = [p, u, \rho, z]^{\mathrm{T}}, \qquad e_1 = [a^2, -a/\rho, 1, 0]^{\mathrm{T}}. \tag{16a}$$

Similarly, the other eigenvectors can be derived as

$$e_2 = [0, 0, 1, 0]^{\mathrm{T}}, \qquad e_3 = [0, 0, 0, 1]^{\mathrm{T}}, \qquad e_4 = [a^2, a/\rho, 1, 0]^{\mathrm{T}}. \tag{16b}$$

With the vectors e_i known, the intermediate points and sonic points can be derived in a number of different ways. The well known method of using Riemann invariants can be used, since there are three Riemann invariants along each of the subpaths. However, for $\gamma_L \neq \gamma_R$ a solution can be obtained only by iteration, since it involves finding the root of

$$ap_*^\alpha + bp_*^\beta = c,$$

where p_* is the pressure at the intermediate states and a, α, b, β and c are functions of U_L and U_R. This is computationally expensive and not an option, since the whole point of using an ARS is to avoid iteration. However, the key observation made in Reference 14 is valid here as well: the intermediate points and sonic points need only be as accurate as the overall discretization error.

If $\Delta\tau_i$ denotes the strength of the ith wave, summing the contributions from all waves gives a linear equation for $\Delta\tau_i$ if the vectors e_i of (16) are constant vectors. Since only a local solution is required, a good approximation is obtained by freezing the vectors e_i at $\bar{V}=(V_i+V_{i+1})/2$. Thus the equation for the strengths can be written as

$$B\cdot\vec{\Delta\tau} = \Delta V = V_{i+1} - V_i, \tag{17}$$

where B is a matrix with $e_i(\bar{V})$ as columns and $\vec{\Delta\tau}$ is a column vector containing $\Delta\tau_i$. A unique solution for the wave strengths exists as long as the vectors e_i are linearly independent, which is when

$$\det(B) = 2a^3/\rho \neq 0.$$

Since this is always true, the wave strengths are unique and are obtained by inverting equation (17). This gives

$$2a^2\Delta\tau_1 = \Delta p - \rho a \Delta u, \tag{18a}$$

$$a^2\Delta\tau_2 = -\Delta p + a^2\Delta\rho, \tag{18b}$$

$$\Delta\tau_3 = \Delta z, \tag{18c}$$

$$2a^2\Delta\tau_4 = \Delta p + \rho a \Delta u. \tag{18d}$$

Once the $\Delta\tau_i$ are known, the intermediate states are obtained as follows. Using the natural order or p-variant, we get

$$V_{i+1/4} = V_i + \Delta\tau_1 e_1, \qquad V_{i+2/4} = V_{i+1/4} + \Delta\tau_2 e_2, \qquad V_{i+3/4} = V_{i+2/4} + \Delta\tau_3 e_3. \tag{19a}$$

In practice, we obtained slightly better results if the same procedure was carried out from V_{i+1} and the average of the two results used. In other words,

$$V_{i+3/4} = V_{i+1} - \Delta\tau_4 e_4, \qquad V_{i+2/4} = V_{i+3/4} - \Delta\tau_3 e_3, \qquad V_{i+1/4} = V_{i+2/4} - \Delta\tau_2 e_2, \tag{19b}$$

and the averages of (19a) and (19b) are used as the intermediate states. Lastly, from equation (15) it follows that the state $V_{i+2/4}$ makes no contribution to $F_{i+1/2}$ and thus need not have been computed. This will be important in the extension to many species.

Next we turn to the determination of the sonic points which may occur on the simple wave paths corresponding to λ_1 and λ_4. The sonic points can be obtained exactly using Riemann invariants, but the calculation involves several exponents. We follow a simpler procedure which works just as well. Assume that conditions are such that a sonic point exists on the wave path corresponding to λ_1 and let the endpoints of this path (which are known conditions) be denoted by the subscritps L and R. The slope of the eigenvalue at the two ends can be calculated as

$$\frac{d\lambda}{d\tau} = \frac{\partial\lambda_1}{\partial V}\cdot e_1. \tag{20}$$

A linear interpolation for the eigenvalue gives

$$\tau_s = \frac{\lambda_L^1}{\lambda_L^1 - \lambda_R^1}, \tag{21}$$

with the sonic point given by

$$V_s = V_L(1-\tau_s) + V_R\tau_s. \tag{22}$$

A more accurate estimate of the sonic point may be obtained by using the slope of the eigenvalue at the endpoints, given by equation (20). While a cubic fit is possible, a parabolic fit is simpler and as effective. A parabolic fit is obtained by solving for τ_s from

$$\lambda_L^1 + \left.\frac{d\lambda^1}{d\tau}\right|_L \tau_s + \left(\lambda_R^1 - \lambda_L^1 - \left.\frac{d\lambda^1}{d\tau}\right|_L\right)\tau_s^2 = 0, \tag{23}$$

with the sonic point given by

$$V_s = V_L + G_L^1\tau_s + (V_R - V_L - G_L^1)\tau_s^2, \tag{24}$$

where G_L^1 is the slope of λ_1 at V_L. In most cases the second-order-accurate formulae gave better results. In some cases, equation (23) would not yield a real solution in the range $0 \leqslant \tau_s \leqslant 1$ and in such cases the linear approximation was used.

5. EXTENSION TO SEVERAL SPECIES

We consider the extension of the results of the two earlier sections to include an arbitrary number of species denoted by n. In realistic hypersonic calculations the chemistry model generally includes a large number of species and it is cumbersome to work with $n+2$ intermediate states. As shown below, only two intermediate states need be computed to obtain $F_{i+1/2}$, leading to an efficient algorithm.

If the primitive variable vector V is defined to be

$$V = [p, u, \rho, z_1, \ldots, z_{n-1}], \tag{25}$$

a linearly independent set of vectors can be taken to be

$$\begin{aligned} e_1 &= [a^2, -a/\rho, 1, 0, \ldots, 0], \\ e_2 &= [0, 0, 1, 0, \ldots, 0], \\ e_3 &= [0, 0, 0, ,1, 0, \ldots, 0], \\ &\vdots \\ e_{n+1} &= [0, 0, 0, 0, 0, \ldots, 1], \\ e_{n+2} &= [a^2, +a/\rho, 1, 0, \ldots, 0]. \end{aligned} \tag{26}$$

Inverting equation (17), we get as before

$$2a^2\Delta\tau_1 = \Delta p - \rho a\Delta u, \tag{27}$$

$$2a^2\Delta\tau_{n+2} = \Delta p + \rho a\Delta u, \tag{28}$$

where, as previously, the coefficients are evaluated at the mean state $\bar{V}$. The two intermediate states, which are the endpoints of the waves corresponding to $u-a$ and $u+a$, can be calculated as

$$V_{i+1/3} = V_i + e_1\Delta\tau_1, \qquad V_{i+2/3} = V_{i+1} - e_{n+2}\Delta\tau_{n+2}, \tag{29}$$

and these are the only intermediate states required to calculate $F_{i+1/2}$ because the eigenvalue u is constant from $V_{i+2/3}$ to $V_{i+1/3}$ and the contributions from the intermediate segments cancel each other. A longer averaging procedure, similar to the one described earlier, may be used here also to obtain slightly better estimates of $V_{i+2/3}$ and $V_{i+1/3}$.

The determination of the sonic points proceeds exactly as described above. The slope of the eigenvalue is calculated by equation (20), which is used for the quadratic approximation.

6. NUMERICAL COMPUTATIONS

In the present study we considered the system of only two species described in Section 3. The Euler equations are integrated using the explicit one-step Lax–Wendroff scheme given by

$$U^{n+1} = U^n + \Delta t U_t^n + \tfrac{1}{2}\Delta t^2 U_{tt}^n, \tag{30}$$

where the time derivatives are replaced by the spatial derivatives and the source term via the Euler equations (8). To obtain a crisp and monotone shock representation, the notion of a TVD scheme, originally due to Harten, can be employed. Many versions based on this idea are available in the literature. The one used here interpolates monotonically the fluxes themselves to the cell faces. Since this procedure is considered to be more or less standard, we shall omit specific details about the second-order extension, which can be found in Reference 17 in great detail. The final expressions that result for U_t and U_{tt} are

$$-(U_t)_i = \frac{1}{\Delta x}(\Delta^+ F_{i-1}^+ + \Delta^+ F_i^-) - S_i - \frac{1}{2\Delta x}\Delta^-(\phi_i^+ \Delta^+ F_i^+ - \phi_{i+1}^- \Delta^+ F_i^-), \tag{31}$$

$$(U_{tt})_i = \frac{1}{\Delta x^2}\Delta^-(\phi_i^+ A_{i+1/2}\Delta^+ F_i^+ + \phi_{i+1}^- A_{i+1/2}\Delta^+ F_i^-) - \frac{1}{2\Delta x}\Delta^-(\phi_i^+ A_{i+1/2} S_{i+1} + \phi_{i+1}^- A_{i+1/2} S_i)$$

$$- G_i \frac{1}{\Delta x}(\Delta^+ F_{i-1}^+ + \Delta^+ F_i^- - S_i \Delta x). \tag{32}$$

The upwind-split flux differences $\Delta^+ F^\pm$ are defined in Section 3. The matrix G_i is the Jacobian of S with respect to U evaluated at x_i and $A_{i+1/2} = (A_i + A_{i+1})/2$.

The first two terms on the RHS of equation (31) are nothing but the first-order upwind formula. Second-order accuracy is then obtained in smooth (non-extremal) regions of the flow by adding the remaining higher-order correction terms, which are suitably limited via so-called limiter functions $\phi^\pm$. Discussion of these limiter functions is outside the scope of this paper and the reader is referred to References 17 and 18. Unless otherwise mentioned, the superbee limiter was used in all calculations. For coarse grids and large source terms, different limiter functions can yield physically different results, as will be shown below. The natural order or the p-variant was used in all calculations.

Non-dimensional units are used throughout the calculation; u_0, L and ρ_0 are reference quantities which non-dimensionalize all other quantities. Note that the non-dimensional reaction rate is none other than the Damkohler number and that $\Delta h/u_0^2$ is the non-dimensional heat release. In all test cases a uniform grid of 200 points was used.

Initial tests with k and Δh set to zero were conducted on ideal gas shock tube problems. The idea in these tests was to determine how large an initial discontinuity could be resolved by the linearized approach described above. Figure 2 shows the results for a shock tube problem with an initial pressure jump of 100, an initial density jump of 30 and zero initial velocity everywhere. It can be seen that the resolution across the shock is excellent, while the resolution across the contact is not as good. A small glitch can also be seen at the site of the original discontinuity,

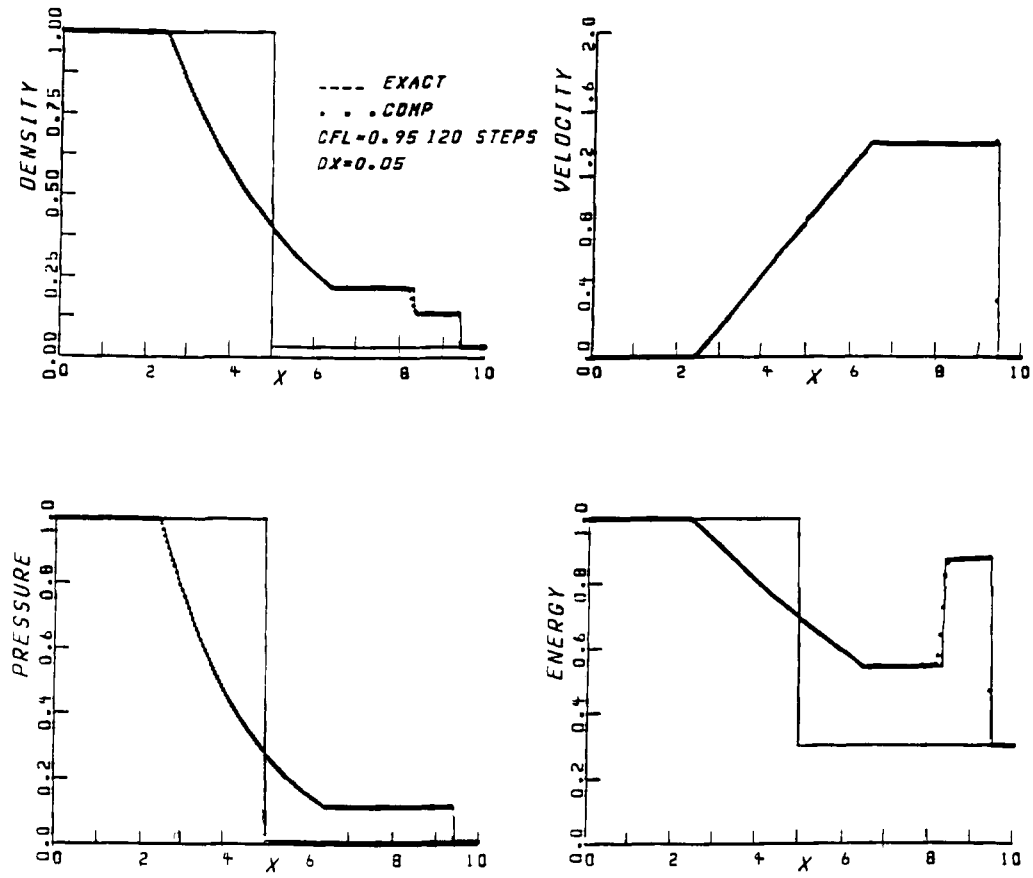

Figure 2. Ideal gas shock tube problem. Frozen solution

indicating that the initial discontinuity is not yet fully resolved. Since this is a fairly extreme shock tube problem, the results suggest that the linearized approach is robust enough to handle most cases.

The next test case is the ozone decomposition ZND detonation case of References 16 and 19, which consists of a moving detonation wave. The detonation wave consists of a shock wave facing the unburnt gas which raises the temperature of the gas beyond the ignition threshold. This initiates the reaction, which results in a monotonic decrease in pressure and density to their equilibrium values. In contrast to the previous case, γ is assumed (perhaps unrealistically) to be constant during the reaction, so that $\gamma(1)=\gamma(0)=1{\cdot}4$. For this example the temperature is defined to be $T=p/\rho$. The reaction rate is of the form

$$k=k_0 z H(T-T_c), \tag{33}$$

where H is the Heavyside step function, which is a simplified form of the Arrhenius law. The other parameters (in CGS units) are

$$\Delta h=-5{\cdot}196\times 10^9, \qquad k_0=5{\cdot}825\times 10^9, \qquad T_c=1{\cdot}155\times 10^9. \tag{34}$$

The initial conditions were taken as follows: for $0 \leqslant x \leqslant 5$,

$$p_1 = 8{\cdot}321 \times 10^5, \qquad \rho_1 = 1{\cdot}201 \times 10^{-3}, \qquad u_1 = 0, \qquad z_1 = 1; \tag{35}$$

for $5 \leqslant x \leqslant 10$,

$$p_2 = 6{\cdot}27 \times 10^6, \qquad \rho_2 = 1{\cdot}945 \times 10^{-3}, \qquad u_2 = 4{\cdot}162 \times 10^4, \qquad z_2 = 0. \tag{36}$$

Under these conditions a detonation wave propagates to the right at a speed $D_{CJ} = 1{\cdot}088 \times 10^5$ cm s^{-1}. In a reference frame fixed to the wave the downstream conditions are sonic and the fluxes of total energy, momentum and mass are the same as upstream. To follow the moving wave, the grid is moved uniformly at D_{CJ}, which means we keep eliminating cells at the left boundary and adding new cells at the right boundary. The boundary conditions at the right are held fixed at upstream values and the boundary conditions at the left are taken to be those of the last eliminated cell.

Colella *et al.*[19] investigated a similar case with second-order Godunov and random choice methods and found that on coarse grids the numerical solution bifurcated from the physically correct strong detonation solution to a non-physical solution consisting of a weak detonation followed by a shock wave. The weak detonation moves at mesh speed—one cell per time

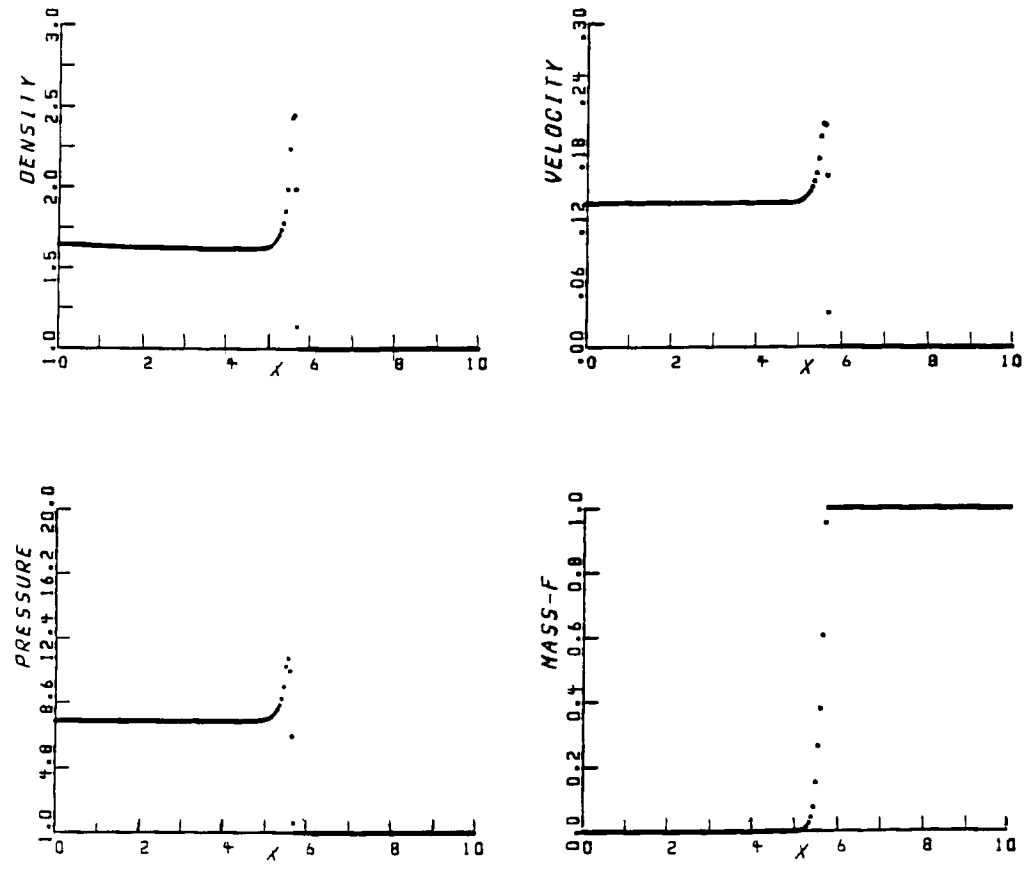

Figure 3. Chapman–Jouguet detonation problem on a fine grid. Reaction zone = 10 cells

step—and is accompanied by complete heat release. On the basis of a simplified scalar model, the authors provide explicit conditions under which a spurious solution exists.

The reaction zone is approximately 5×10^{-5} cm and for a fine grid simulation $\Delta x = 5 \times 10^{-6}$ cm and $\Delta t = 5 \times 10^{-12}$ s. These were the same values as used in Reference 16 for case 2a. The results after 2000 iterations are shown in Figure 3. The ZND spike is clearly resolved, though the pressure peak is about 3% lower than the approximate peak value quoted in Reference 4. One reason for this discrepancy is that our TVD approximation is only first-order-accurate at smooth extrema. Other than for this small discrepancy, our results compare well with those presented in Reference 16.

Figure 4 presents results for the coarse grid case, where the reaction zone is approximately one-tenth of a cell. Here $\Delta x = 5 \times 10^{-4}$ cm and $\Delta t = 10^{-10}$ s, which correspond to case 4a of Reference 16. The results after 10000 iterations are shown in Figures 4(a) and 4(b) using the superbee and van Leer limiters respectively. It can be seen that the superbee limiter gives the correct CJ solution while the van Leer limiter gives the spurious weak detonation solution. This somewhat surprising result verifies the theoretical results of Reference 19 in that spurious non-physical solutions exist on coarse grids. Aside from this, our results also seem to be smoother than those obtained in Reference 16.

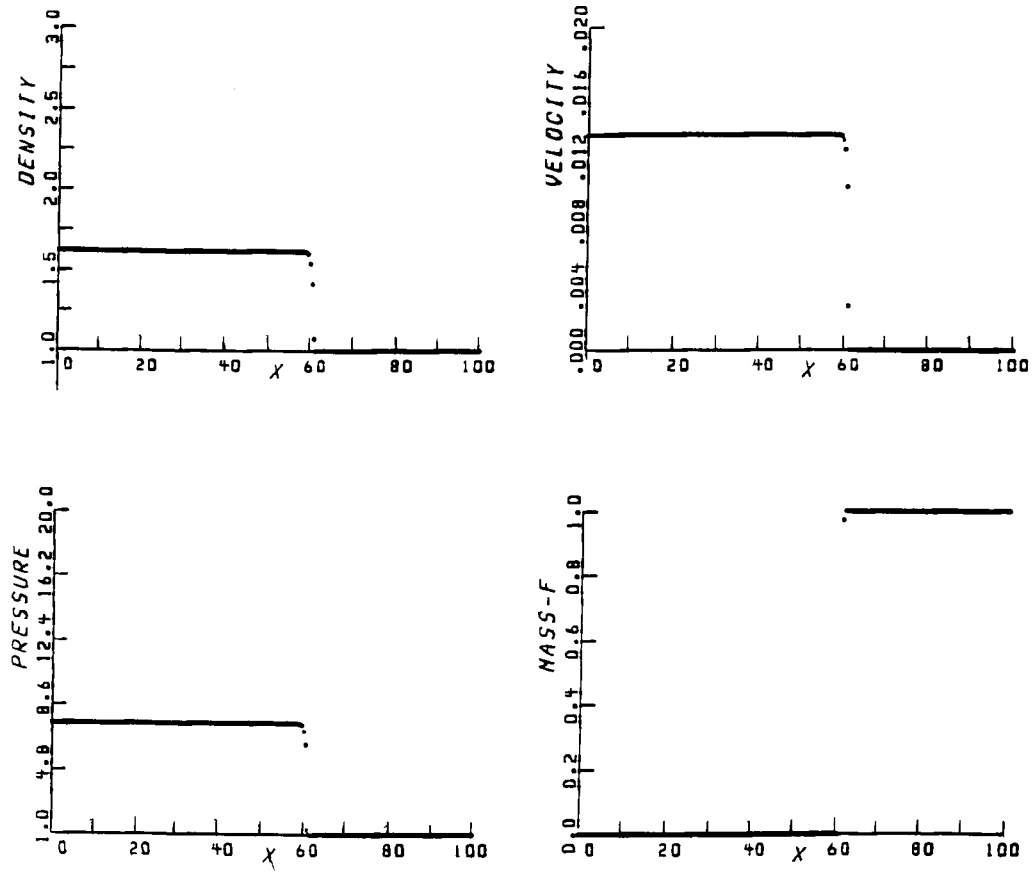

Figure 4(a). Chapman–Jouguet detonation problem on a coarse grid. Reaction zone = 1/10 cell, superbee limiter

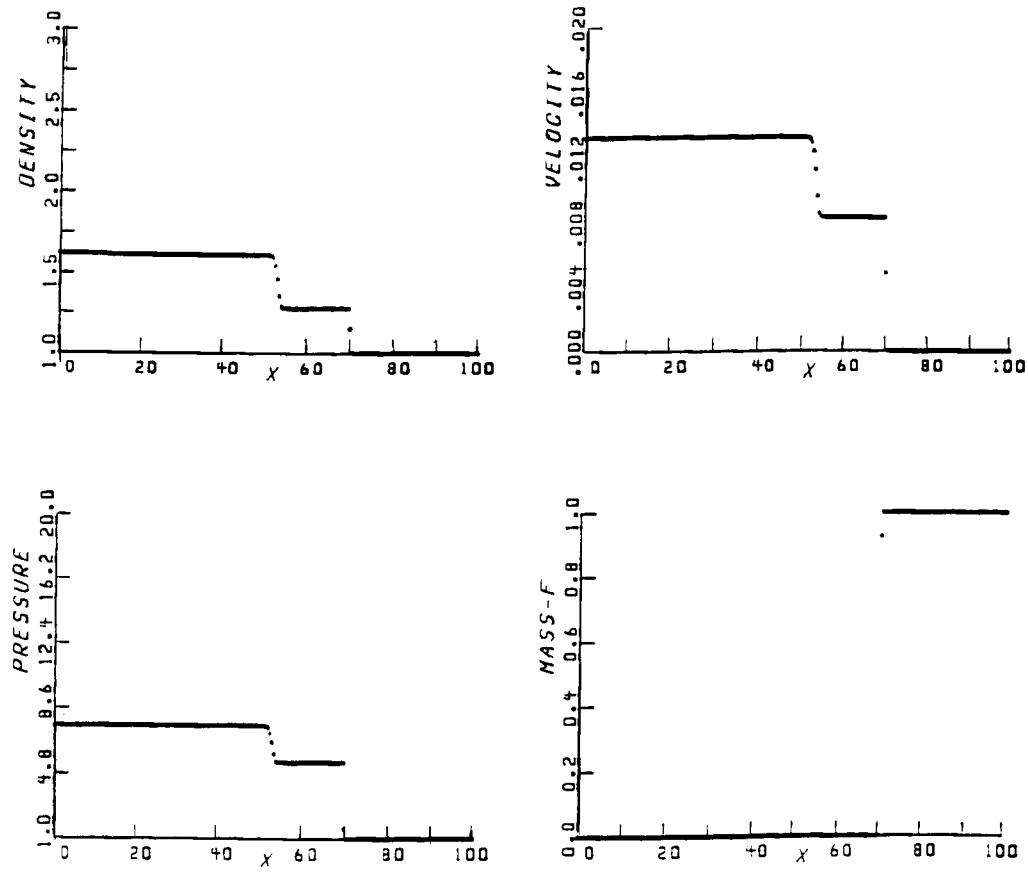

Figure 4(b). Chapman–Jouguet detonation problem on a coarse grid. Reaction zone = 1/10 cell, van Leer limiter.

Before proceeding to the next test case, we would like to make several comments about the results obtained above. To confirm that the results observed were not due to the approximations used in determining the intermediate and sonic points, we performed the coarse grid computations using exact Riemann invariants. The results were identical to those presented above. In addition, the first-order upwind scheme also gave the spurious weak detonation solution, which suggests that the spurious solution is obtained with the more dissipative schemes. Lastly, if the problem is solved in a reference frame moving with the detonation wave, the spurious solution is not observed.

The last test case consists of steady flow through a divergent nozzle with an imbedded normal shock. For this case the source term in equation (8) is

$$S = -\frac{A_x}{A}[\rho u, \rho u^2, \rho Eu + pu, \rho uz]^T + [0, 0, 0, -\rho k]^T. \tag{37}$$

The flow is frozen upstream of the shock and shock-induced reactions take place downstream of it. The area distribution is given by

$$A(x) = 2{\cdot}0 + 0{\cdot}2x, \quad 0 \leqslant x \leqslant 10. \tag{38}$$

The inflow Mach number was chosen so that the throat area was unity. Since the inflow is supersonic, all primitive variables were prescribed at inflow. At outflow the static pressure was prescribed and the other primitive variables were extrapolated. The value of the exit pressure was chosen so that in the frozen case the upstream shock Mach number was 2·5. The frozen solution was used as the initial condition for the computations.

The following non-dimensional parameters were used:

$$\gamma(0)=1{\cdot}6, \qquad \gamma(1)=1{\cdot}4, \qquad \Delta h=-1{\cdot}0, \qquad k_0=1{\cdot}0. \tag{39}$$

The reaction rate is given by equation (33) with the ignition temperature $T_c=1{\cdot}12T_0$, where T_0 is the static temperature of the gas at inflow.

The computed profiles of internal energy (total internal energy e), pressure, velocity and mass fraction are shown in Figure 5. Also shown for comparison is the frozen solution. The non-equilibrium solution shows a weaker normal shock followed by a fairly large reaction zone, leading to equilibrium, conditions at the exit. While an 'exact' solution to this problem is tedious, two analytical integrals are immediately available. These were found to be essentially constant over the length of the nozzle, confirming the accuracy of the computed numerical solution. The steady shock is resolved in two intermediate points. If the nozzle is viewed as a supersonic engine inlet, the example illustrates the role of combustion in promoting 'inlet unstarts'.

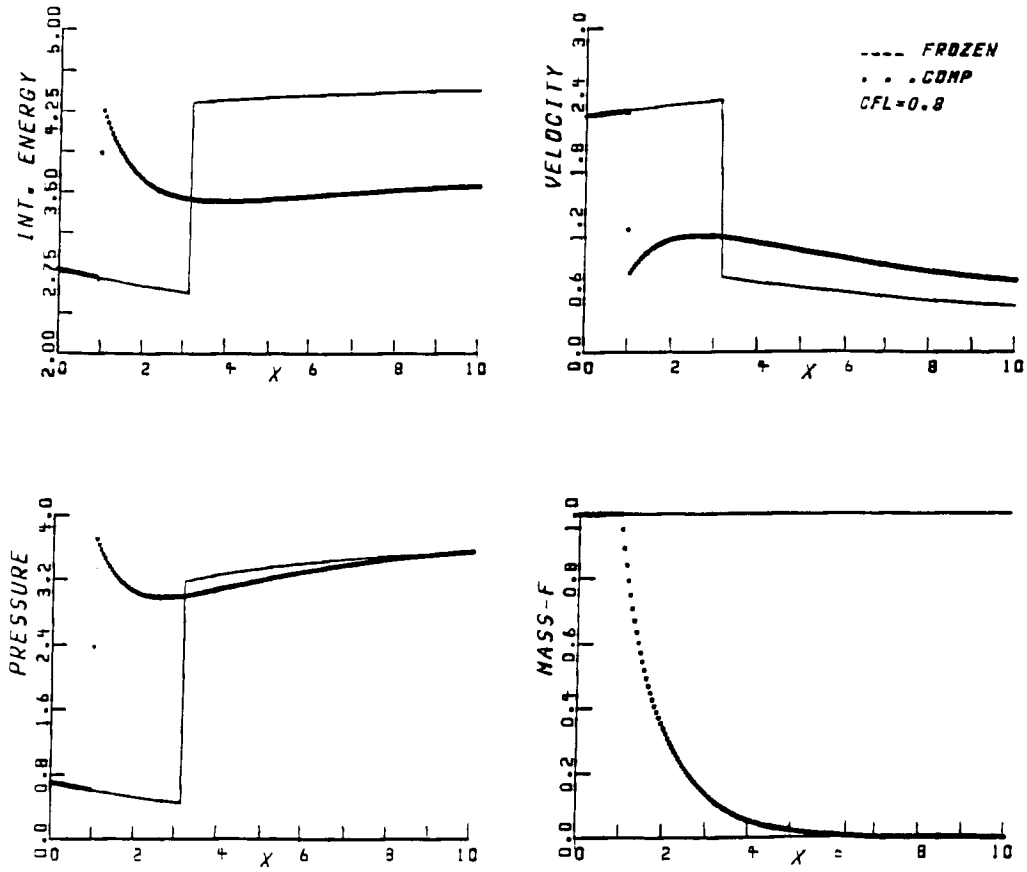

Figure 5. Divergent nozzle problem. Reaction zone = 20 cells.

7. CONCLUSIONS

In this paper we have presented an efficient extension of the Osher scheme to non-equilibrium reacting flows and applied the scheme to several reacting flow problems. The extension proceeds by using a Riemann solver for the homogeneous system and adding in the effects of the source terms explicitly. The method has the advantage that no iteration is required to find the intermediate states. Computational results for several test problems have confirmed the robustness, efficiency and accuracy of the scheme.

On coarse grids it was observed that a change of limiter triggered a change from a CJ detonation solution to a spurious weak detonation solution. It would be very interesting to see whether some type of splitting of the source terms might ensure that the physically correct solution is obtained in all cases. This is, however, beyond the scope of this paper.

ACKNOWLEDGEMENTS

The first author was supported by the NASA Lewis Research Center under contract NAS-25266 with Dr. T. J. Benson as monitor. The authors would like to thank Dr. M. S. Raju for several illuminating discussions.

REFERENCES

1. S. K. Godunov, *Mat. Sbornik*, **47**, 271 (1959).
2. J. L. Steger and R. F. Warming, *J. Comput. Phys.*, **40**, 263 (1981).
3. B. van Leer, *Lecture Notes in Physics, Vol. 170*, Springer, New York, 1982, p. 507.
4. P. L. Roe, *J. Comput. Phys.*, **43**, 357 (1981).
5. S. Osher, *Mathematical Studies, Vol. 47*, North-Holland, Amsterdam, 1981, p. 179.
6. S. Osher and F. Solomon, *Math. Comput.*, **38**, 339 (1982).
7. B. Engquist and S. Osher, *Math. Comput.*, **36**, 321–352 (1982).
8. T. W. Roberts, *J. Comput. Phys.*, **90**, 141–160 (1990).
9. P. Glaister, *J. Comput. Phys.*, **74**, 382 (1988).
10. M. S. Liou, B. van Leer and J. S. Shuen, *J. Comput. Phys.*, **87**, 1 (1990).
11. B. Larrouturou and L. Fezoui, in Carasso, Charrier, Hanouzet and Joly (eds), *Nonlinear Hyperbolic Problems, Lecture Notes in Mathematics*, Springer, Heidelberg, 1989.
12. J. S. Shuen, M. S. Liou and B. van Leer, *J. Comput. Phys.*, **90**, 371 (1990).
13. M. Vinokur and J. L. Monatgne, *J. Comput. Phys.*, **89**, 276 (1990).
14. A. Suresh and M. S. Liou, *AIAA J.*, **29**, 920 (1991).
15. R. J. LeVeque and H. C. Yee, *J. Comput. Phys.*, **86**, 187–210 (1990).
16. M. Ben-Artzi, *J. Comput. Phys.*, **81**, 70–101 (1989).
17. M.-S. Liou, *AIAA Paper 87-0355*, 1987.
18. P. K. Sweby, *SIAM J. Numer. Anal.*, **21**, 995 (1984).
19. P. Colella, A. Majda and V. Roytburd, *SIAM J Sci. Stat. Comput.*, **7**, 1059 (1986).